
Proceedings Paper:
Luo, P., Madathil, S.N.E., Nishizawa, S.-I. et al. (2020) Dynamic avalanche free super junction-TCIGBT for high power density operation. In: 2020 32nd International Symposium on Power Semiconductor Devices and ICs (ISPSD). 2020 32nd International Symposium on Power Semiconductor Devices and ICs (ISPSD), 13-18 Sep 2020, Vienne, Austria (online). IEEE. ISBN: 9781728148373. ISSN: 1063-6854. EISSN: 1946-0201.

https://doi.org/10.1109/ispsd46842.2020.9170129

Dynamic Avalanche Free Super Junction-TCIGBT for High Power Density Operation

Peng Luo, Sankara Narayanan Ekkanath Madathil
Department of Electronic and Electrical Engineering
The University of Sheffield
Sheffield, United Kingdom
pluo2@sheffield.ac.uk

Shin-ichi Nishizawa, and Wataru Saito
Research Institute for Applied Mechanics
Kyushu University
Fukuoka, Japan

***Abstract*—Dynamic Avalanche (DA) effects in the Super-Junction Trench IGBTs are analyzed through 3-D TCAD simulations for the first time. A DA free solution for high power density and low loss is proposed and demonstrated in detail. Furthermore, simulation results show that DA results in significant increase in turn-off losses in the Super-Junction Trench IGBTs at high current density operations, which poses a fundamental limit on the power density of IGBT applications. In contrast, the Super-Junction Trench Clustered IGBTs remain DA free at high current density and show low switching losses due to enhanced PMOS action. Therefore, the Super-Junction Trench IGBTs are well suitable for high power density operations with a potential to operate beyond the 1-D unipolar 4H-SiC limit.**

Keywords—IGBT; CIGBT; dynamic avalanche; high current density; super junction

I. INTRODUCTION

Recent development of new silicon IGBT designs targets enhancing operating current densities and switching frequencies with an aim to reduce system costs for various power electronic applications [1]. It is crucial to implement novel technologies into IGBTs in order to continuously improve the E_{off}-$V_{ce(sat)}$ trade-off. Recently, several novel approaches to improve on-state performance by the enhancement of emitter side carrier density have been demonstrated [2-4]. The resulting on-state carrier density is typically in the range of 10^{16} to 10^{17} cm^{-3}, which is at least two or three orders of magnitude higher than the background doping concentration (N_D). During turn-off, the stored carriers can result in a peak electric field (E_{max}) which is much higher than the off-state electric field strength, as depicted in Fig. 1. As electric field crowds beneath trench gates, the E_{max} appears at trench bottom rather than at the P-base/N-drift junction. If the resulting E_{max} exceeds the concentration dependent critical electric field (E_{cr}), Dynamic Avalanche (DA) will be triggered even when the collector voltage is well below the off-state breakdown voltage. More excess carriers are thus generated to increase E_{off}. In addition, excess carriers generated due to Impact Ionization (I.I.) can have enough energy to be injected into the trench oxide to affect the gate stability. Therefore, DA can fundamentally limit the operating current density, switching frequency, turn-off loss and reliability of MOS-bipolar devices. Tremendous efforts have been devoted to suppressing, but not eliminating DA in trench IGBTs to ensure safe operation and high robustness in emerging electric transport

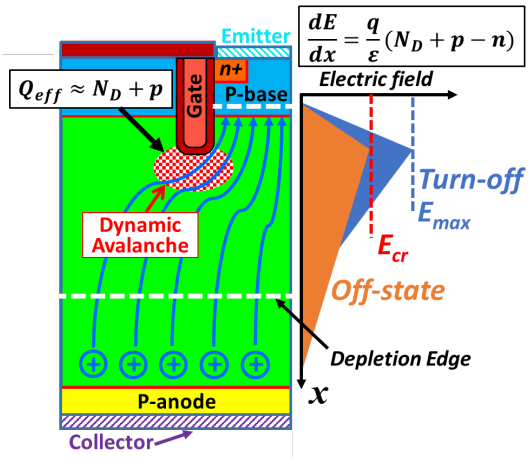

Fig. 1. Schemetic of DA in the turn-off of TIGBT.

applications. More recently, a 1.2 kV DA free design has been demonstrated in a Trench Clustered IGBT (TCIGBT) through simulations and experiments [5]. Due to absence of DA, the TCIGBT can be operated with very low power losses at high current densities without associated reliability concerns. Moreover, it was shown that Super-Junction (SJ) concept can further improve the E_{off}-$V_{ce(sat)}$ trade-off in TCIGBTs due to the unique PMOS structure, which connects to the p-pillars in the drift region to effectively extract the excess carriers from the bulk during turn-off [6]. Such an option does not exist in IGBTs.

This paper aims to clarify the DA effects in the Super-Junction Trench IGBT (SJ-TIGBT) for the first time through 3-D TCAD simulations [7]. A DA free SJ-TCIGBT is proposed for ultra-high current density and frequency operations, with a potential to operate beyond the 1-D unipolar 4H-SiC limit.

II. DA IN SJ-TIGBT AND A DA FREE SOLUTION: SJ-TCIGBT

The circuit configuration used to analyze the inductive switching behavior is shown in Fig. 2. Fig. 3 shows the 3-D cross-sections of a 1.2 kV SJ-TIGBT and a 1.2 kV SJ-TCIGBT in field-stop technology. Main structural parameters are kept identical and pillars charges are set as 1.2e12 cm^{-2}. Both devices are switched-off at a load current of 100 A with identical current density (200 A/cm^2) and on-state voltage drop conditions.

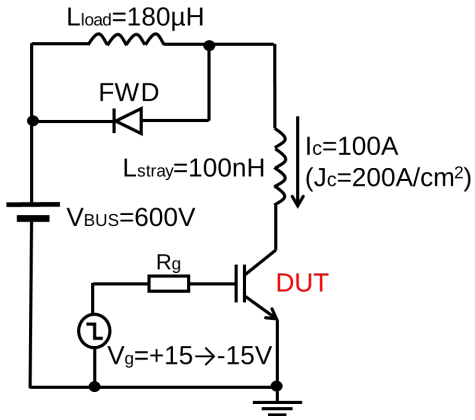

Fig. 2. Test circuit configuration for inductive switching.

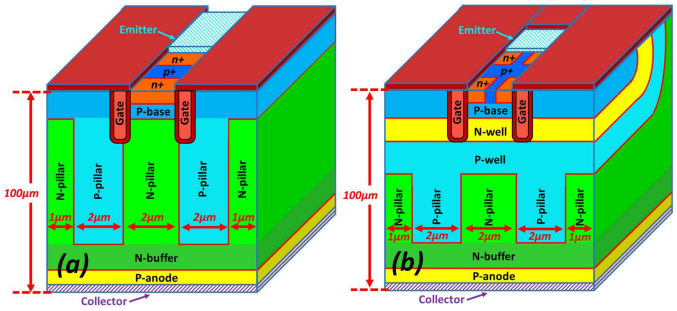

Fig. 3. 3-D cross-sectional views of (a) SJ-TIGBT and (b) SJ-TCIGBT. (SJ depth=90 μm, pillars charge: Q_n=Q_p=1.2e12 cm^{-2})

A. Comparison of Turn-off Characteristics

The simulated turn-off characteristics of SJ-TIGBT and SJ-TCIGBT as a function of gate resistance (R_g) are shown in Fig. 4 and Fig. 5, respectively. In practice, using small R_g can be a direct method to speed up turn-off due to high dI/dt. However, the turn-off curves of SJ-TIGBT show a decreasing trend of surge voltage when $R_g < 20\ \Omega$. This indicates the occurrence of DA within the device and results in a low dI/dt as well as a saturated trend of E_{off} at small R_g, as shown in Fig. 6. In comparison, the turn-off curves of SJ-TCIGBT shows a continuous increase in surge voltage with decrease in R_g due to higher dI/dt, which is an evidence to show the DA free performance of SJ-TCIGBT. Hence, the E_{off} shows a linear decrease with reduction in R_g values and is much lower than that of SJ-TIGBT due to PMOS action. The detailed turn-off process of SJ-TCIGBT can be explained using Fig. 7. During device turn-off, the gate bias is switched to -15 V and an inversion layer will be formed in the N-well layer along the trench wall-side. The PMOS structure which consists of P-base/N-well/P-well turns on and provides a direct path for excess holes to evacuate. Due to self-clamping voltage, the body potential of the PMOS increases to turn the PMOS into on-state. Therefore, it is not necessary to use negative gate voltages to turn-on the PMOS so that the off-state gate voltages have no influence on the E_{off}, as shown in Fig. 6. Moreover, the p-pillars act as the extension of P-well layer, which help collect the excess holes within the thick N-drift region. It can be seen that excess holes only flow within p-pillars and finally evacuate through PMOS structure. Therefore, the SJ-TCIGBT shows a higher dI/dt in comparison to that of SJ-TIGBT and high switching frequency operation can

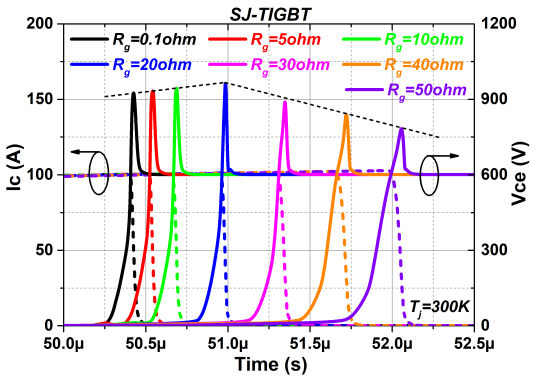

Fig. 4. Simulated turn-off characteristics of SJ-TIGBT at various R_g.

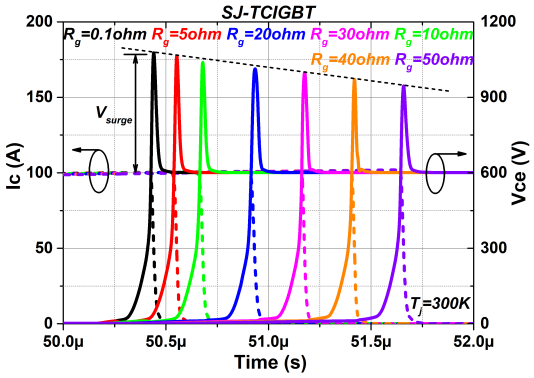

Fig. 5. Simulated turn-off characteristics of SJ-TCIGBT at various R_g.

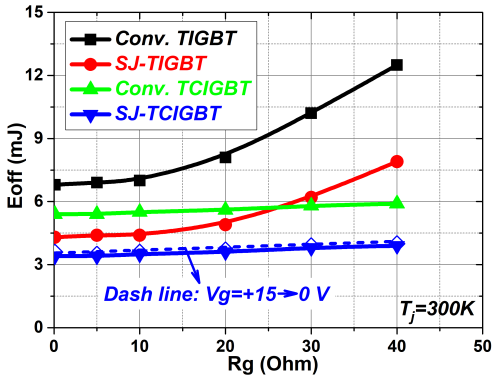

Fig. 6. Influence of R_g on E_{off} of conventional TIGBT, conventional TCIGBT, SJ-TIGBT and SJ-TCIGBT, respectively. (Same $V_{ce(sat)}$ condtion)

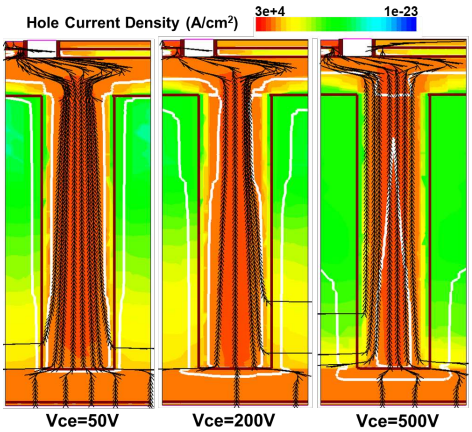

Fig. 7. Hole current density distribution within SJ-TCIGBT during switch-off at various collector voltages.

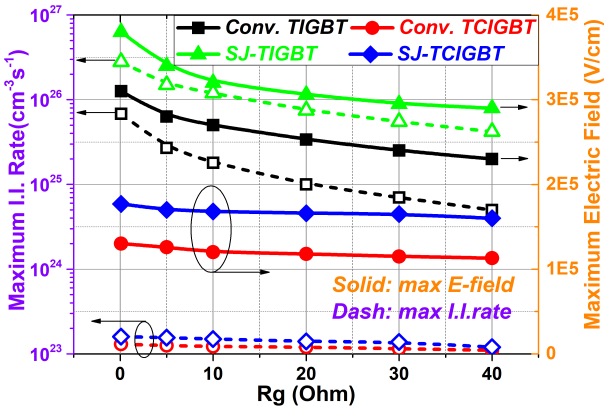

Fig. 8. Influence of R_g on E_{max} and I.I. rates of the TIGBT, TCIGBT, SJ-TIGBT and SJ-TCIGBT when V_{ce} increases to 600V during turn-off, respectively. (J_c=200 A/cm^2)

be realized. In addition, the high surge voltages can be reduced by increasing P-anode doping concentration without significant influence on current tails [6], and the P-anode injection efficiency has no influence on DA [5].

B. *Comparison of DA Performacne*

Fig. 8 shows the comparison of maximum electric fields (E_{max}) and maximum Impact Ionization (I.I.) rates at the time point of V_{ce} increases to 600 V during turn-off. In comparison to the conventional TIGBT, the DA is even further enhanced in the SJ-TIGBT. This is because that the E_{max} which appears at the bottom of the trench gates is modulated by the effective net charge ($Q_{eff} \approx N_D + p$) around trench corners. Higher Q_{eff} will result in a higher E_{max}. As shown in Fig. 9, due to high N-pillar donor concentration (N_D = 6e15 cm^{-3}), the SJ-TIGBT presents significantly higher E_{max} as well as significant increases in I.I. rates compared to that of conventional TIGBT. Therefore, the enhanced DA performance limits the reduction of E_{off} at small R_g in the SJ-TIGBT, although the lower E_{off} compared with the conventional TIGBT can be obtained by fast removal of excess carriers through P-pillars as shown in Fig. 6. In contrast, due to self-clamping feature and effective PMOS actions of TCIGBT and SJ-TCIGBT, the trench bottoms are protected from high electric fields as the collector voltage is supported by the P-well/N-pillar junction. Hence, the SJ-TCIGBT does not suffer from DA, and has the lowest E_{off} amongst the four devices considered herein.

III. High Current Density and Low Loss Operation

The continuous increase of power density is crucial for the development of IGBTs to achieve design optimization and low cost for converter systems. Higher power density requires higher operating current density and low loss per chip area. Fig. 10 shows the simulated I-V characteristics of the SJ-TCIGBT while Fig. 11 shows the turn-off waveforms as a function of R_g at J_c = 500 A/cm^2. Due to thyristor conduction, the SJ-TCIGBT shows a $V_{ce(sat)}$ of 1.7 V at 500 A/cm^2 at 25 ºC. Moreover, the SJ-TCIGBT remains DA free behavior at high current density operation. Fig. 12 compares the E_{off} between SJ-TIGBT and SJ-TCIGBT at J_c = 500 A/cm^2. Due to the influence of DA, the SJ-

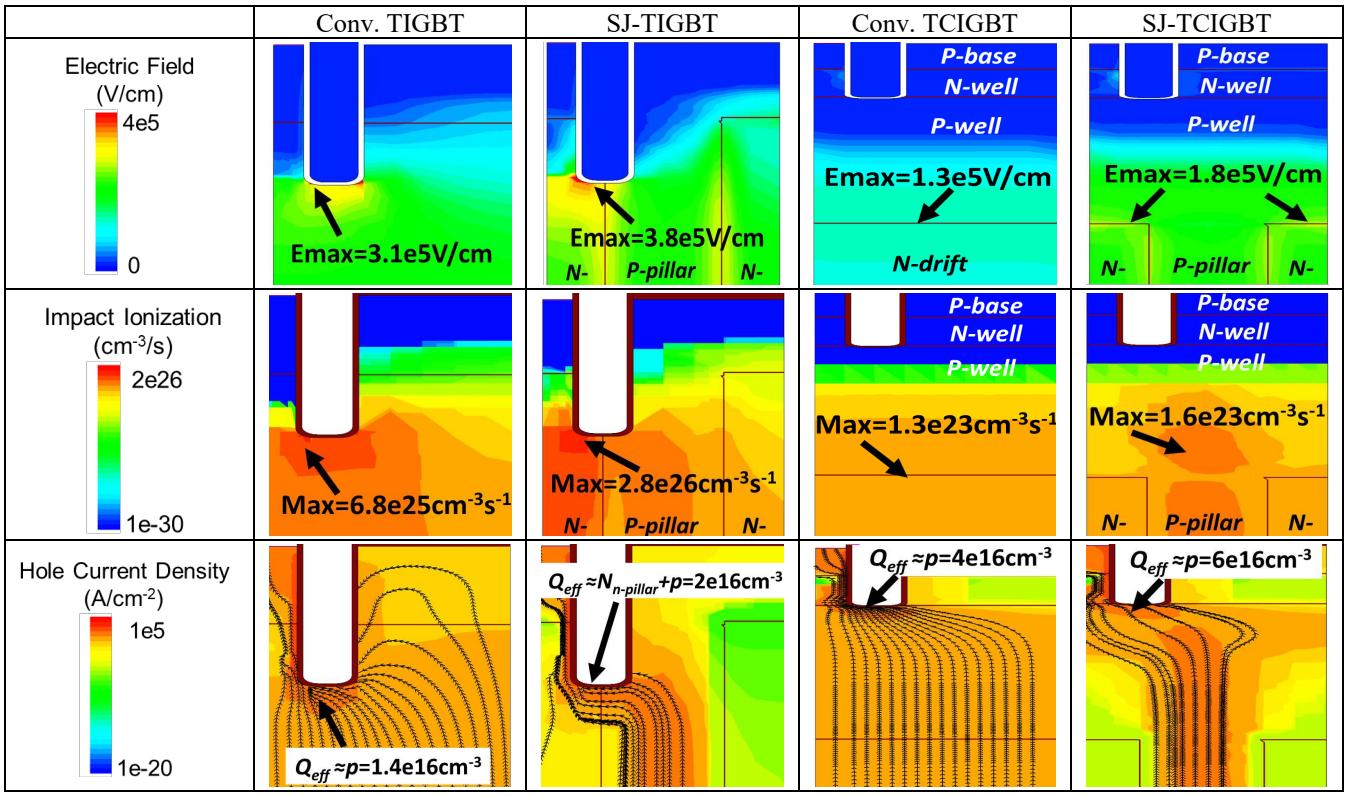

Fig. 9. Comparison of (a) E-field distributions, (b) I.I. rates and (c) net charge densities, respectively. (J_c = 200 A/cm^2, R_g = 0.1 Ω, V_{ce} = 600 V).

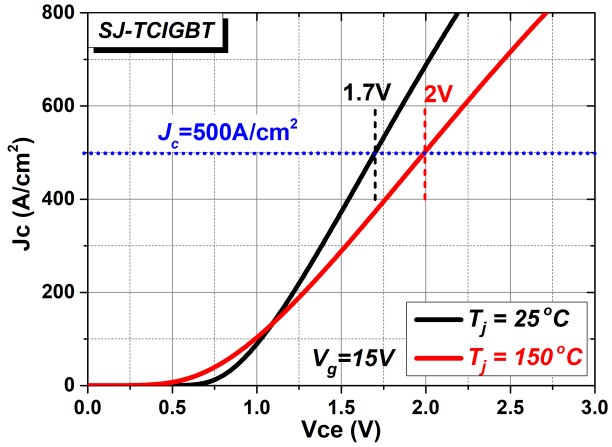

Fig. 10. Simualted I-V characteristics of the SJ-TCIGBT at T_j = 25 ºC and T_j = 150 ºC.

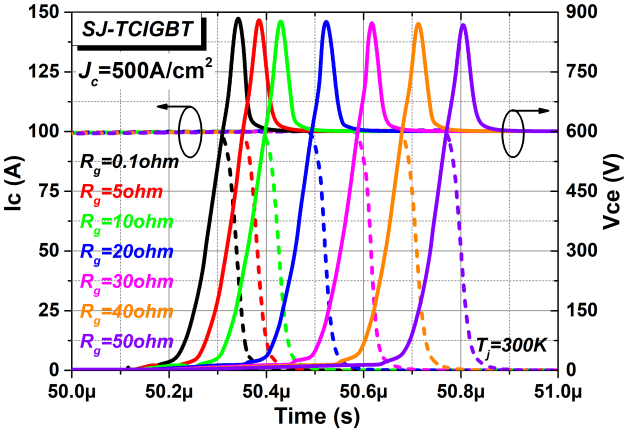

Fig. 11. Simulated turn-off waveforms as a function of R_g of SJ-TCIGBT at J_c = 500 A/cm^2.

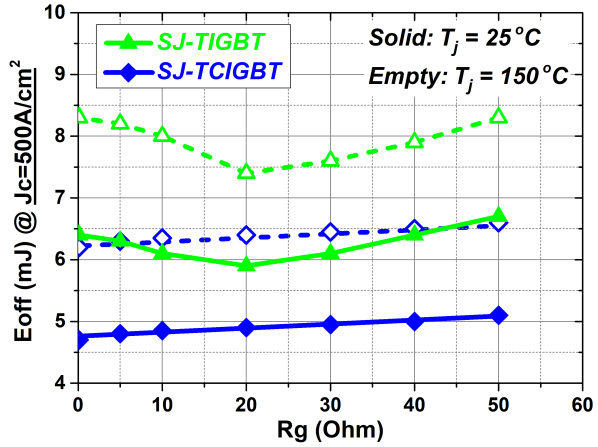

Fig. 12. Comparison of E_{off} between SJ-TIGBT and SJ-TCIGBT at J_c = 500A/cm^2.

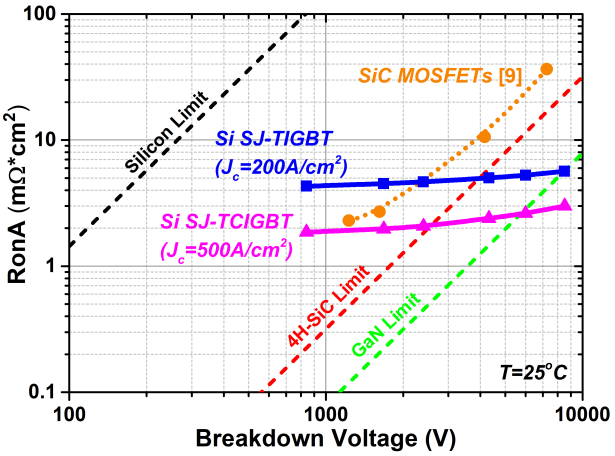

Fig. 13. Theoretical on-state performance limits of silicon SJ-TIGBT at J_c= 200 A/cm^2 and silicon SJ-TCIGBT at J_c= 500 A/cm^2 at T_j = 25 ºC.

TIGBT even shows a slight increase in E_{off} when R_g < 20 Ω, which significantly limits the reduction of E_{off}. In contrast, owing to the DA free performance of SJ-TCIGBT, the E_{off} is only 3.4 mJ at R_g = 0.1 Ω at R.T., which is 27 % lower than that of the SJ-TIGBT at same $V_{ce(sat)}$ condition. More importantly, the high current density operation capability of SJ-TCIGBT enables the on-state performance limit of silicon IGBTs to outperform the performance of commercial SiC MOSFETs [8] and the 4H-SiC 1-D unipolar limit when BV > 2.5 kV at J_c = 500 A/cm^2, as shown in Fig. 13.

IV. Conclusions

The DA effects in the 1.2 kV SJ-TIGBTs are analyzed for the first time. A DA free operation with low switching losses is demonstrated in the SJ-TCIGBT. The unique self-clamping feature can effectively protect the trench gates and avoid electric field crowding effects during switch-off. Furthermore, simulation results show that the SJ-TCIGBT is well suited for high current density and low loss operation without DA effects. Finally, the SJ-TCIGBTs enable the on-state performance of silicon IGBTs to outperform SiC MOSFETs and exhibit a potential to outperform 1-D unipolar 4H-SiC limit.

References

[1] K. Vogel, J. Baurichter, O. Lenze, U. Nolten, A. Philippou, *et al.*, "New, best-in-class 900-A 1200-V EconoDUAL™ 3 with IGBT 7: highest power density and performancend performance," in *PCIM Europe*, pp. 1-8, May 2019.

[2] C. Jaeger, A. Philippou, A. V. Ilei, J. G. Laven, and A. Härtl, "A new sub-micron trench cell concept in ultrathin wafer technology for next generation 1200 V IGBTs," in *Proc. ISPSD'17*, pp. 69-72, May 2017.

[3] K. Kakushima, T. Hoshii, K. Tsutsui, A. Nakajima, S. Nishizawa, *et al.*, "Experimental verification of a 3D scaling principle for low Vce(sat) IGBT," in *IEDM'16,* pp. 10.6.1-10.6.4, Dec. 2016.

[4] M. Sumitomo, J. Asai, H. Sakane, K. Arakawa, Y. Higuchi, *et al.*, "Low loss IGBT with Partially Narrow Mesa Structure (PNM-IGBT)," in *Proc. ISPSD'12*, pp. 17-20, Jun. 2012.

[5] P. Luo, S. N. E. Madathil, S. Nishizawa, and W. Saito, "Dynamic Avalanche Free Design in 1.2kV Si-IGBTs for Ultra High Current Density Operation," in *IEDM'19*, pp. 12.3.1-12.3.4, Dec. 2019.

[6] N. Luther-King, M. Sweet, and E. M. S. Narayanan, "Clustered Insulated Gate Bipolar Transistor in the Super Junction Concept: The SJ-TCIGBT," *IEEE Trans., Power Electronics,* vol. 27, 2012, pp. 3072-3080.

[7] I. Synopsys, Sentaurus Device User Guide: Ver. L-2017. 09.

[8] J. W. Palmour, "Silicon carbide power device development for industrial markets," in *IEDM'14,* pp. 1.1.1-1.1.8, Dec. 2014.